

Estimating covariant Lyapunov vectors from data

Cite as: Chaos **32**, 033105 (2022); <https://doi.org/10.1063/5.0078112>

Submitted: 10 November 2021 • Accepted: 15 February 2022 • Published Online: 04 March 2022

 Christoph Martin, Nahal Sharifi and  Sarah Hallerberg



[View Online](#)



[Export Citation](#)



[CrossMark](#)

ARTICLES YOU MAY BE INTERESTED IN

[Anticipating synchrony in dynamical systems using information theory](#)

Chaos: An Interdisciplinary Journal of Nonlinear Science **32**, 031103 (2022); <https://doi.org/10.1063/5.0079255>

[Understanding the origins of the basic equations of statistical fibrillatory dynamics](#)

Chaos: An Interdisciplinary Journal of Nonlinear Science **32**, 032101 (2022); <https://doi.org/10.1063/5.0062095>

[Quantifying the robustness of a chaotic system](#)

Chaos: An Interdisciplinary Journal of Nonlinear Science **32**, 033124 (2022); <https://doi.org/10.1063/5.0077645>

[LEARN MORE](#)

APL Machine Learning

Open, quality research for the networking communities

MEET OUR NEW EDITOR-IN-CHIEF



Estimating covariant Lyapunov vectors from data

Cite as: Chaos **32**, 033105 (2022); doi: [10.1063/5.0078112](https://doi.org/10.1063/5.0078112)

Submitted: 10 November 2021 · Accepted: 15 February 2022 ·

Published Online: 4 March 2022



View Online



Export Citation



CrossMark

Christoph Martin, Nahal Sharifi, and Sarah Hallerberg^{a)}

AFFILIATIONS

Department of Mechanical Engineering and Production Management, Hamburg University of Applied Sciences, Berliner Tor 21, 20099 Hamburg, Germany

^{a)}Author to whom correspondence should be addressed: christoph.martin@haw-hamburg.de

ABSTRACT

Covariant Lyapunov vectors characterize the directions along which perturbations in dynamical systems grow. They have also been studied as predictors of critical transitions and extreme events. For many applications, it is necessary to estimate these vectors from data since model equations are unknown for many interesting phenomena. We propose an approach for estimating covariant Lyapunov vectors based on data records without knowing the underlying equations of the system. In contrast to previous approaches, our approach can be applied to high-dimensional datasets. We demonstrate that this purely data-driven approach can accurately estimate covariant Lyapunov vectors from data records generated by several low- and high-dimensional dynamical systems. The highest dimension of a time series from which covariant Lyapunov vectors are estimated in this contribution is 128.

Published under an exclusive license by AIP Publishing. <https://doi.org/10.1063/5.0078112>

Lyapunov exponents (LEs) are well-known measures of chaos. They determine the growth rate of perturbations along different directions. Covariant Lyapunov vectors (CLVs) serve as a basis to these exponents and provide us with the corresponding directions of perturbation growth in a dynamical system.¹ Additionally, CLVs have been proposed as predictors of critical transitions^{5,6} and long-lasting weather conditions.⁸ So far, CLVs in high-dimensional systems could effectively only be computed if the exact evolution equations of the system are available.^{9–12} In this paper, we propose a new approach for estimating CLVs from data in the absence of any knowledge of the underlying equations. Using sparse identification of nonlinear dynamics,¹⁵ we estimate the Jacobian matrices from trajectories of different high- and low-dimensional dynamical systems from data. We demonstrate that these estimated Jacobians can be employed to estimate CLVs, the full Lyapunov spectrum, and finite-time Lyapunov exponents (FTLEs) from data even in the presence of noise. Being able to infer CLVs from data records might encourage numerous future applications in data analysis and data-based predictions.

I. INTRODUCTION

CLVs¹ indicate the unstable and stable directions of dynamical systems. As an intrinsic basis for Lyapunov exponents, they provide crucial information about the dynamical structure of a system, and

they form a precious tool for studying perturbation growth, coupling, and predictability in chaotic systems.^{2–6} CLVs have also been employed in the context of data-assimilation for weather and climate models.⁷ Tangencies of CLVs are reported to be predictors for extreme events and critical transitions^{5,6} and to be linked to weather instabilities.⁸

So far, the usage of CLVs was, however, limited to problems for which knowledge of the underlying equations of the system^{9–12} was available, i.e., systems for which realistic models exist. More specifically, two conditions must be addressed for the use of CLVs in a data-driven scenario without knowing the underlying equations: CLVs have to be computed without knowing the far future of the system, and they have to be computed from data without the knowledge of the underlying equations. Sharifi *et al.*⁶ addressed the first issue by proposing a method to compute approximations of CLVs without knowing the far future of the system. A solution for the latter problem that can be applied to multi-variate time series of arbitrarily high-dimension (as they occur in various applications) was so far missing—this contribution proposes a method to bridge this gap.

One previous contribution¹³ proposed to estimate CLVs through phase-space reconstruction of systems with effective dimensions of two and three. The method proposed in Ref. 13 is, however, not reported to be employed in applications, and a generalization to high-dimensional systems was so far missing. The reason for this is most likely the fact that phase-space reconstruction is

typically limited to low-dimensional systems since reconstruction of high-dimensional systems would require enormously large data records, which are typically not available in realistic application scenarios. Recently, in a related context (estimation of optimally time-dependent modes), a combination of phase-space reconstruction and training of artificial neural networks has been suggested.¹⁴ In this contribution, we propose a conceptually different approach for estimating CLVs from data based on the sparse identification of nonlinear dynamics (SINDy).¹⁵ We demonstrate that Jacobians estimated using a modified version of SINDy can be utilized to estimate CLVs from data records of low- and high-dimensional dynamical systems. In this proof-of-concept study, we use complete datasets with a relatively high sampling frequency, as they are currently collected using modern sensors and storage methods in many different applications. Since we are testing whether the method is able to produce good estimates of CLVs at all, we do not address more specific issues, such as missing data, working in the limit of very short datasets and unknown dimensions of the system in this study.

More specifically, we present the method for estimating CLVs in Sec. II and discuss how to evaluate the quality of all estimated quantities in Sec. III. We then test our approach using trajectories of a low-dimensional chaotic system (Lorenz system)¹⁶ (see Sec. IV), a system exhibiting critical transitions (Josephson junction)¹⁷ (see Sec. V), and high-dimensional spatiotemporal chaotic systems (Lorenz 96)¹⁸ of dimensions $n = 32, 64$, and 128 (see Sec. VI). We discuss the robustness of the proposed approach in the presence of added noise in Sec. VII and present conclusions in Sec. VIII.

II. ESTIMATING COVARIANT LYAPUNOV VECTORS FROM DATA

Computing CLVs for a particular dynamical system

$$\frac{d}{dt}\mathbf{x} = \mathbf{f}(\mathbf{x}, t) \quad (1)$$

requires the knowledge of the tangent operator, i.e., in numerical applications the Jacobian $J_{i,j} = \frac{\partial f_i(\mathbf{x}, t)}{\partial x_j}$, with $1 \leq i, j \leq n$ and n denoting the dimension of the system. Attempts to estimate the Jacobian or the leading Lyapunov exponent from data exist for a long time.^{19–24} Here, we use a modified version of an algorithm for the sparse identification of nonlinear dynamics (SINDy).¹⁵ To facilitate understanding, we first summarize the idea of SINDy. The observed state of a system at discrete times $t = 1, 2, \dots, T$ is denoted by \mathbf{x}_t , the matrix with all observed states by $\mathbf{X} = [\mathbf{x}_1, \mathbf{x}_2, \dots, \mathbf{x}_T]^\top$. The respective time derivatives of these states computed using central finite differences²⁵ are stored in the matrix $\dot{\mathbf{X}} = [\dot{\mathbf{x}}_1, \dot{\mathbf{x}}_2, \dots, \dot{\mathbf{x}}_T]^\top$. We then create the feature matrix (also called the library) $g(\mathbf{X})$ to model the nonlinearities in the dynamics by applying several transformations to the data. For example, $g(\mathbf{X}) = [\mathbf{1}, \mathbf{X}, \mathbf{X}^2, \dots, \sin(\mathbf{X}), \dots]$, with the notation referring to operations being performed elementwise. If the underlying dynamics are unknown, the library can include features computed by many different families of functions. The parts of the library that are effectively contributing to the dynamics are then chosen using a sparse encoding approach. To find a sparse solution for $\dot{\mathbf{X}} = g(\mathbf{X})\mathbf{B}$, we refer to

Ref. 26 for a detailed analysis of the convergence properties of this algorithm. Other techniques for variable selection and regularization (e.g., lasso²⁷) could also be deployed during this step. Note that the nonzero entries of \mathbf{B} indicate the relevant terms for the dynamics of the system, and thus, using $\mathbf{B}^\top g(\mathbf{x}^\top)^\top$, we can approximate $\frac{d}{dt}\mathbf{x}$ [as in Eq. (1)] for each row of the data record \mathbf{X} . If the algorithm does not yield a sparse \mathbf{B} , the feature matrix likely does not cover the appropriate functions and thus might need to be extended. In some scenarios, other variations of the SINDy algorithm might be preferable.²⁸ In applications, however, a suitable set of candidate functions of the library has to be identified within a preselection step by testing which candidate-functions or sets of functions provide good hindcasts of the observed datasets. The selected candidate functions (or their derivatives) could then form the set of functions employed in the estimation of Jacobians.

Utilizing the model derived from data, we compute numerical partial derivatives to approximate $\frac{\partial f_i(\mathbf{x})}{\partial x_j}$, which constitute the approximated Jacobian $\hat{\mathbf{J}}$ using a central finite difference method with 4th order accuracy.²⁵ This procedure enables us to approximate Jacobians from data records without the knowledge of the underlying equations. Section VII provides an analysis of the estimation errors. In the following, we demonstrate that these estimated Jacobians are so close to their equation-based analogs that we can use them to estimate CLVs. This is surprising since computing finite differences on any quantity estimated from data is typically a source of high numerical noise.

III. EVALUATING THE QUALITY OF ALL ESTIMATED QUANTITIES

We test the method proposed above by applying it to several well-known dynamical systems. For each system under study, we create datasets of simulated trajectories that we then consider as data records. Based on these trajectories, we then estimate the Jacobians at each point in time using the procedure explained above. The estimated Jacobians are then employed to compute several dynamical indicators: CLVs, Lyapunov exponents, and finite-time Lyapunov exponents. We compare the CLVs computed using estimated Jacobians (in the following referred to as *data-based CLVs* and *data-based Jacobians*) to the corresponding CLVs computed using the model equations (in the following referred to as *equation-based CLVs* and *equation-based Jacobians*) by measuring differences in angle. Additionally, we employ two different algorithms to compute CLVs: the algorithm of Ginelli *et al.*¹¹ and the approximative near-future method (NFM).⁶

We employ three different time steps while computing the trajectory, the Jacobian matrix, and the CLVs. In the first step, we use a time step of δt to numerically integrate Eq. (1) to obtain the trajectory. In all our models, we use $\delta t = 0.0005$. We then interpret the simulated trajectories as examples for data records and use SINDy to estimate the Jacobians for each time step. In the next step, we use the estimated Jacobians to determine the evolution of perturbations to the trajectory using either Ginelli's algorithm or the NFM. Therefore, we use a Runge–Kutta method for iteration of the perturbation vectors, and as a result, the time step is increased to $2\delta t$, i.e., 0.001 . We also reorthogonalize the perturbation vectors every Δt . In the

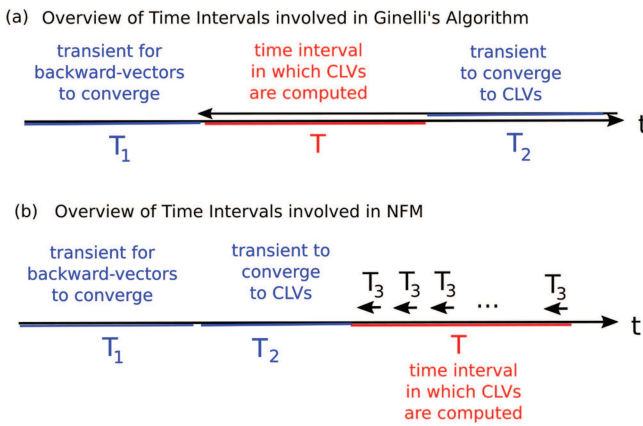


FIG. 1. Schematic overview of time intervals involved in the computation of CLVs using (a) Ginelli's algorithm and (b) the near-future method.

case of the Lorenz model and the Josephson junction $\Delta t = 0.01$, i.e., we reorthogonalize every $20 \delta t$ steps. As for the Lorenz 96 model, Δt is increased to 0.1.

During the computation of the CLVs employing Ginelli's method, we need to have a transient of length T_1 for a forward iteration of the perturbation vectors in order for them to converge to the backward vectors (see Fig. 1 for a schematic overview of time intervals). We also need a transient of length T_2 for a backward iteration of the perturbation vectors from the future. In our low-dimensional models, both T_1 and T_2 are 100. For the Lorenz 96 model, however, we increased the length of both transients to 500. For the NFM method, both T_1 and T_2 are in the past. In the case of our low-dimensional systems, $T_1 = 100$ and $T_2 = 50$. As for the case of Lorenz 96, $T_1 = 500$ and $T_2 = 100$. The NFM then uses a short interval for backward iterations from the future T_3 . This interval is 0.1 for the Lorenz attractor and the Josephson junction and $T_3 = 1$ in the Lorenz 96 model.

We then measure the difference between data-based CLVs and equation-based CLVs generated using Ginelli's algorithm by computing the angles θ_i between the i th data-based and the i th equation-based vector, with $i = 1, 2, \dots, n$ and n denoting the dimension of the system. Analogously, we denote the difference in angle between data-based and equation-based CLVs computed via NFM as ϕ_i with i specified as above. If the vectors coincide, the angle between them is zero or 180 and the absolute value of the cosine of the angle is unity.

Additionally, we compare Lyapunov exponents l_i computed using data-based Jacobians and equation-based Jacobians as well as time series of the corresponding finite-time Lyapunov exponents (FTLEs) λ_i , with $i = 1, 2, \dots, n$ as above.

IV. RESULTS FOR THE LORENZ ATTRACTOR

The estimation of CLVs in low-dimensional dynamical systems is tested using the Lorenz attractor,¹⁶ the prototype model of

a chaotic system given by

$$\begin{aligned}\dot{x} &= \gamma(y - x), \\ \dot{y} &= x(\rho - z) - y, \\ \dot{z} &= xy - \beta z,\end{aligned}\quad (2)$$

with $\beta = 8/3$, $\gamma = 10$, and $\rho = 28$. We integrate the equations of motion numerically and save the resulting Jacobians and trajectories. The simulated trajectories [Fig. 2(a)] are in this context interpreted as *data records*, which we use to test our estimation procedure. We then estimate data-based Jacobians on the basis of these data records and compute LEs, FTLEs, and CLVs using the Ginelli algorithm and the NFM.

As can be seen in Fig. 2(b), LEs estimated from data are close to LEs computed using the Jacobians from differential equations of the model. The exact values of the LEs from data and from model equations are listed in Table I. While the relative error in the first and third LE are quite low, Table I, the second LE suffers from a high relative error. This is to be expected since the second LE, i.e., the average value of the second FTLE, is almost zero and any deviation will result in a high relative error. In both cases, LEs are computed using Benettin's algorithm²⁹ and the data-based Jacobian or the equation-based Jacobian. The FTLEs can also be recovered from data as can be seen in Figs. 2(c)–2(e). The comparison of the angles between data-based and equation-based CLVs is presented in Fig. 2(f). For all three CLVs, the absolute value of the cosine of the angle is most of the time very close to one, indicating that the vectors are tangent. Figure 2(g) displays the corresponding results using the NFM. Similar to Fig. 2(f), the vectors estimated from data are tangent to the ones computed using model equations ($|\cos \theta_i| \approx 1$;

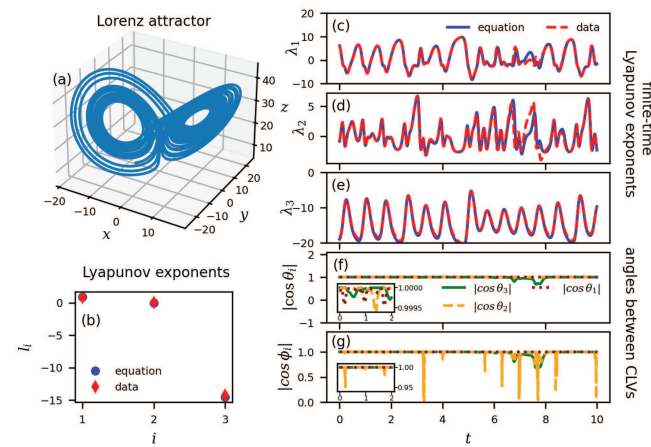


FIG. 2. Approximations of CLVs, LEs, and FTLEs estimated from trajectories of the Lorenz attractor are very close to the respective quantities computed from model equations. (a) Trajectory of the system. (b) LEs computed from model equations compared to LEs estimated from data. (c)–(e) Time series of data-based estimates of FTLEs compared to FTLEs computed from model equations. (f) Absolute value of the cosine of the angle between data-based and equation-based CLVs, both computed using Ginelli's algorithm. (g) Similar to (f) with both sets of CLVs estimated using the NFM.

TABLE I. Values of the LEs using Jacobians derived from model-equations are compared to those computed using Jacobians estimated from data for the Lorenz attractor (σ indicates the level of noise) and the Josephson junction system.

Exponent	System				
	Lorenz attractor				Josephson junction
	($\sigma = 0$)	($\sigma = 1$)	($\sigma = 3$)	($\sigma = 5$)	
l_1	Equation	0.904 228	0.807 743	0.690 658	0.802 638
	Data	0.858 717	0.797 669	0.749 367	1.004 400
	Relative error	0.050 331	0.012 471	0.085 005	0.251 374
l_2	Equation	-0.002 274	0.064 286	-0.039 490	-0.197 828
	Data	0.040 707	0.095 679	0.142 713	0.123 730
	Relative error	18.898 792	0.488 332	4.613 907	1.625 441
l_3	Equation	-14.568 620	-14.538 700	-14.317 830	-14.271 480
	Data	-14.282 820	-14.423 660	-13.606 380	-12.162 020
	Relative error	0.019 618	0.007 913	0.049 690	0.147 809

$i = 1, 2, 3$). Note that the results for the Ginelli algorithm are slightly better than for the NFM. Since the NFM is an approximation of the Ginelli approach using less data from the future, this observation is conclusive.

In order to demonstrate that the time series in Fig. 2 refer to typical results, we also estimated histograms of angles between data-based and equation-based CLVs and histograms of FTLE estimation errors. These histograms (see Figs. 10 and 11) were estimated on the basis of estimated and computed quantities for 12 000 time steps and are visible in Sec. VII within a discussion of the robustness of the proposed method.

V. RESULTS FOR A FAST-SLOW SYSTEM

In order to test our approach on trajectories from a nonlinear dynamical system exhibiting critical transitions and dynamics on different time scales, we choose a model of Josephson junctions^{17,30} given by

$$\begin{aligned} \beta \varepsilon \dot{\phi} &= \psi - (1 + \beta \varepsilon) \phi, \\ \varepsilon \dot{\psi} &= u - \hat{\alpha}^{-1} \phi - \sin \phi, \\ \dot{u} &= J - \sin \phi, \end{aligned} \quad (3)$$

with $\hat{\alpha}^{-1} = 0.2$, $J = 1.5$, $\varepsilon = 0.01$, and $\beta = 0.2$. This three-dimensional model has been used as a prototype model for dynamical systems with fast-slow dynamics and critical transitions.⁶

Integrating the model equations numerically, we obtain a trajectory of a Josephson junction with transitions as is presented in Fig. 3(a). We estimate Jacobians based solely on the trajectory using SINDY and compute the LEs, FTLEs, and CLVs as explained above. As presented in Figs. 3(b)–3(e), data-based estimates of LEs and FTLEs are very close to the respective equation-based quantities. The exact values of the LEs from data and from model-equations as well as their relative errors are depicted in Table I. Data-based CLVs are also tangent to equation-based CLVs [Fig. 3(f)]; i.e., the absolute values of the cosines of the angles between data-based and equation-based CLVs are close to unity. We observe the analog behavior for

CLVs estimated using the near-future method [Fig. 3(g)]. While Figs. 3(c)–3(g) contain only a short interval of the estimated CLVs and FTLEs, Fig. 4 presents the distribution of the angles and relative FTLE errors estimated on the basis of estimates for 50 000 time steps. The distribution of the absolute value of the cosine of the angles between the data-based and equation-based CLVs is presented in Fig. 4(a). The sharp peaks denote that the three CLVs are always approximately tangent using both Ginelli and NFM methods. Furthermore, Fig. 4(b) presents the error of the data-based FTLEs

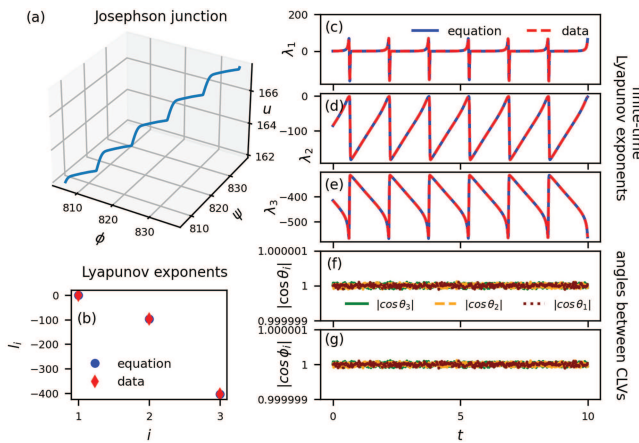


FIG. 3. Approximations of CLVs, LEs, and FTLEs estimated from trajectories of the model for Josephson junctions are very close to the respective quantities computed from model equations. (a) Trajectory of the model for Josephson junctions with transitions. (b) Data-based estimates of LEs compared to LEs computed from model equations. (c)–(e) Time series of data-based estimates of FTLEs compared to FTLEs computed from model equations. (f) Absolute value of the cosine of the angle between data-based and equation-based CLVs, both computed using Ginelli's algorithm. (g) Similar to (f) with both sets of CLVs estimated using the NFM.

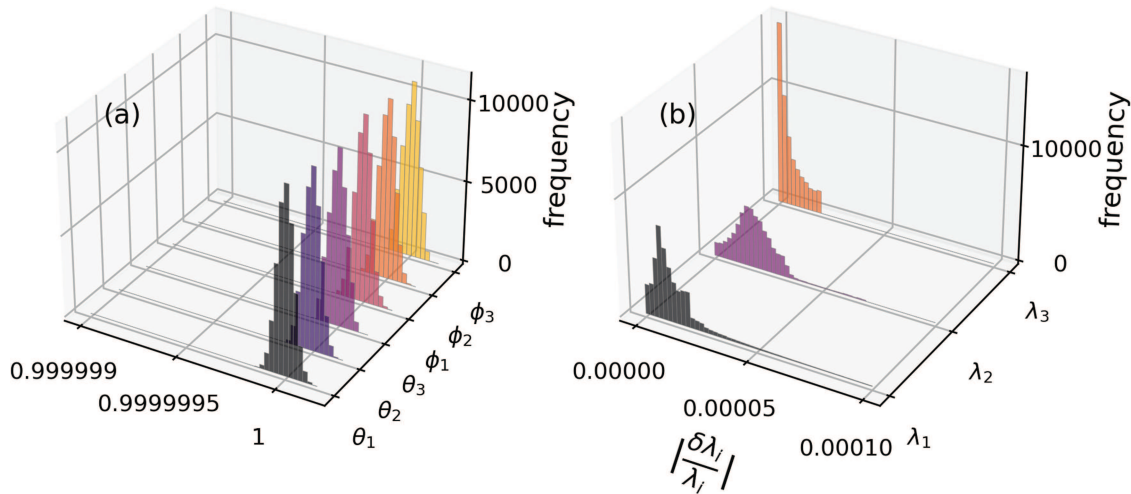
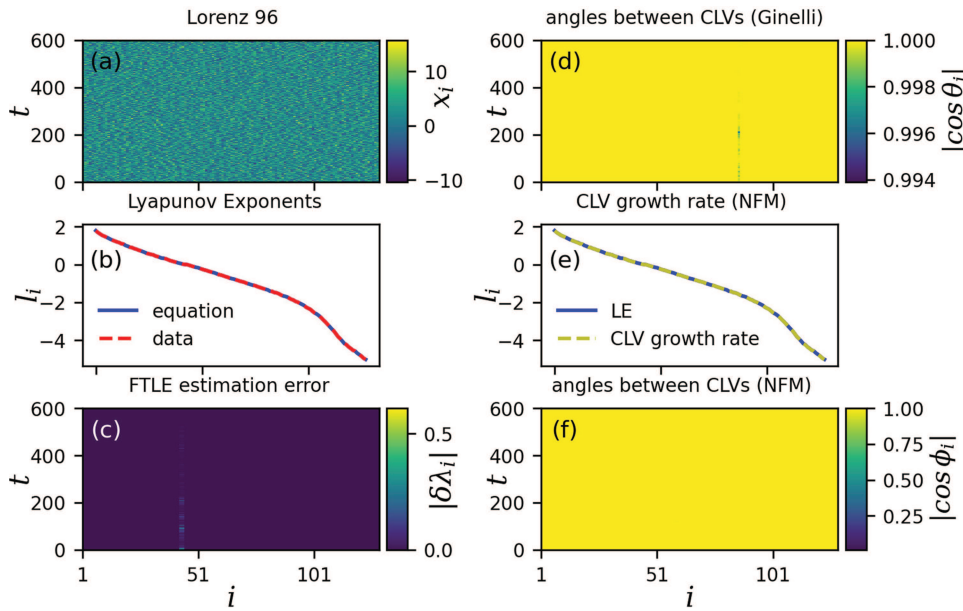


FIG. 4. The distribution of the absolute value of the cosine of the angles between CLVs from model equations and CLVs estimated from data of the Josephson junction. (b) Distribution of the error of the estimated FTLEs as compared to FTLEs obtained from model equations.

as compared to the model-based FTLEs. Note that the absolute values of differences between estimated and equation-based FTLEs $\|\hat{\lambda}_i(t) - \lambda_i(t)\|$ are divided by the absolute value of the equation based FTLE, with $\hat{\lambda}_i(t)$ representing FTLEs estimated from data and $\lambda_i(t)$ denoting FTLEs computed from model equations. Considering the histograms in Fig. 4, we observe that the time series presented in Fig. 3 represent a typical result and not a carefully selected part of the trajectory for which the algorithm works particularly well.



VI. RESULTS FOR A HIGH-DIMENSIONAL SPATIOTEMPORAL CHAOTIC SYSTEM

As an example for a high-dimensional multivariate chaotic time series, we simulate trajectories of Lorenz 96 models¹⁸ given by

$$\dot{x}_i = -x_{i-2}x_{i-1} + x_{i-1}x_{i+1} - x_i + F, \quad (4)$$

with $F = 8$ (for which the system is chaotic), $i = 1, 2, \dots, n$, with cyclic indices, i.e., $x_{n+1} = x_1$, and dimensions $n = 32$, $n = 64$, and

FIG. 5. CLVs can also be estimated from time series of high-dimensional chaotic systems. Lorenz 96 system with $n = 128$ and $F = 8$. (a) Trajectories of the systems. (b) Data-based estimates of LEs compared to LEs computed from model equations. (c) Time series of the differences between data-based estimates of FTLEs and equation-based FTLEs. (d) Absolute value of the cosine of the angle between data-based and equation-based CLVs. Ginelli's method has been used to compute both sets of the CLVs. (e) LEs compared to the average growth rate of the CLVs estimated from the near future, both computed from model equations in order to test the NFM. (f) Similar to (d) with both sets of CLVs estimated using the NFM.

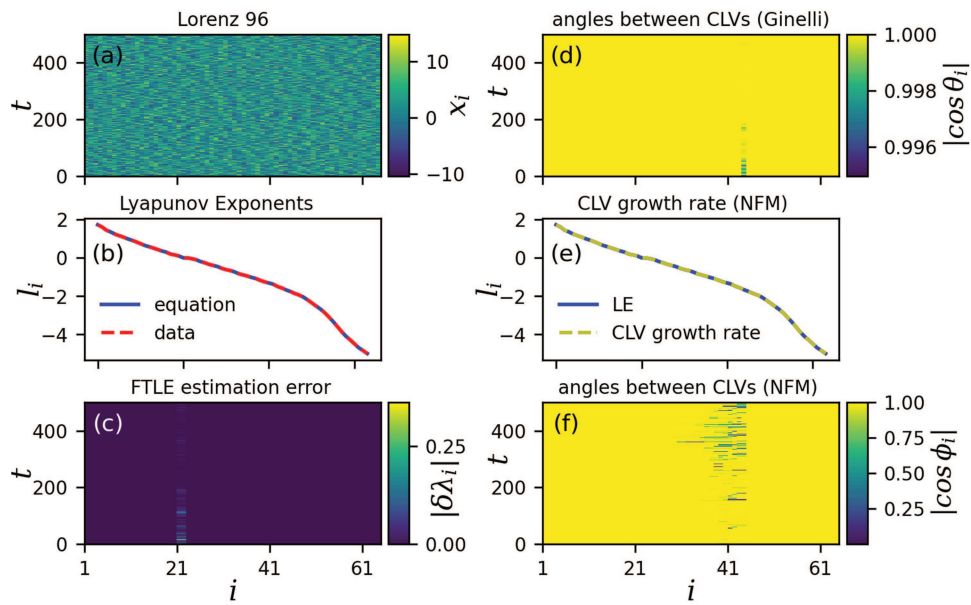


FIG. 6. Data-based and equation-based quantities for a Lorenz 96 system with $n = 64$ and $F = 8$. (a) Trajectories of the systems. (b) Data-based estimates of LEs compared to LEs computed from model equations. (c) Time series of the differences between data-based estimates of FTLEs and equation-based FTLEs. (d) Absolute value of the cosine of the angle between data-based and equation-based CLVs. Ginelli's method has been used to compute both sets of the CLVs. (e) LEs compared to the average growth rate of the CLVs estimated from the near future, both computed from model equations in order to test the NFM. (f) Similar to (d) with both sets of CLVs estimated using the NFM.

$n = 128$. The resulting high-dimensional time series are then utilized to estimate Jacobians and all derived quantities. The observed estimation errors of the Jacobians are very small. For example, in the case of $n = 128$, we compute the Frobenius norm of the difference

between the actual \mathbb{J} and the approximated $\hat{\mathbb{J}}$ for every time step (on the same trajectory) to evaluate the error of the approximation. Over all time steps, the mean (standard deviation) of the error is 3.2×10^{-9} (1.2×10^{-10}).

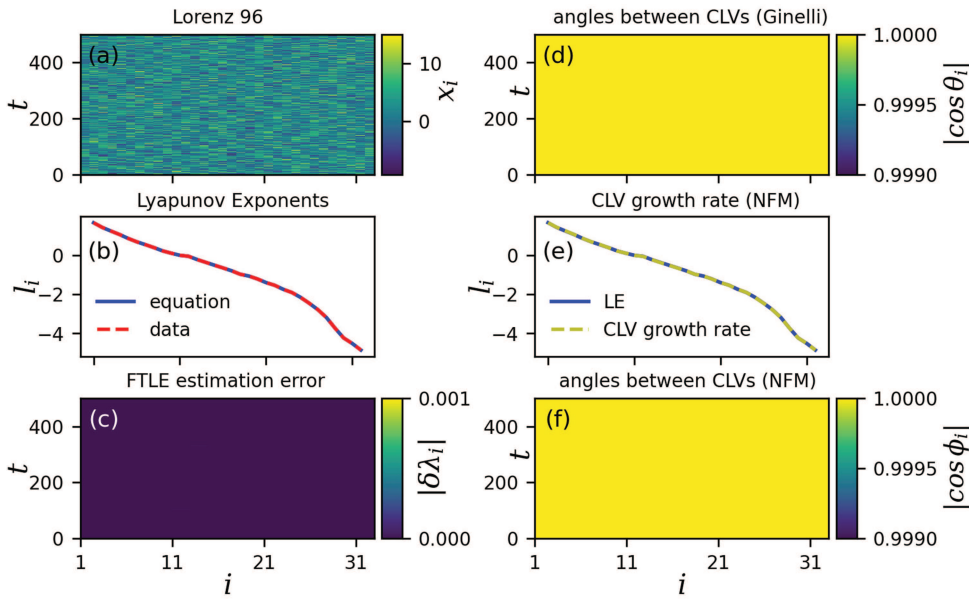


FIG. 7. Data-based and equation-based quantities for a Lorenz 96 system with $n = 32$ and $F = 8$. (a) Trajectories of the systems. (b) Data-based estimates of LEs compared to LEs computed from model equations. (c) Time series of the differences between data-based estimates of FTLEs and equation-based FTLEs. (d) Absolute value of the cosine of the angle between data-based and equation-based CLVs. Ginelli's method has been used to compute both sets of the CLVs. (e) LEs compared to the average growth rate of the CLVs estimated from the near future, both computed from model equations in order to test the NFM. (f) Similar to (d) with both sets of CLVs estimated using the NFM.

The trajectory of a Lorenz 96 model with dimension 128 is presented in Fig. 5(a). Data-based estimates of the Lyapunov spectrum and the Lyapunov spectrum computed from model equations are presented in Fig. 5(b). The estimation error of the FTLEs is presented in Figs. 5(c). Angles between data-based and equation-based CLVs are presented in Fig. 5(d) using Ginelli's algorithm and Fig. 5(f) using the NFM. The data-based CLVs are also almost tangent to the equation-based CLVs. To verify the effectiveness of the NFM for higher dimensions, we also compare the average growth rate of the resulting vectors to the LEs. As can be seen in Fig. 5(e), the average growth rate of the vectors computed using the NFM coincides with the LEs, and therefore, these vectors can be used as a reliable basis for LEs. Results for Lorenz 96 models with 64 and 32 dimensions are conclusive with the 128 dimensional case and are presented in Figs. 6 and 7. We previously observed a lower quality of the estimated vectors for intermediate values of i , which improved to the results presented in Figs. 5–7. More precisely, some deviations of CLVs were observed for intermediate values of i and persisted in time only for a certain while before they dissolve. Using the NFM, the persistence in time was not observed, but deviations were spread among neighboring CLVs for intermediate values of i . A similar but less pronounced effect is still visible in Fig. 6. The quality of estimated CLVs has, however, improved by increasing the length of the transients T_1 to the values, which are specified in Sec. III. This indicates that the accuracy of estimated CLV depends on the length of the available data records. We have not observed this dependence on the length of the transients for lower-dimensional systems since convergences in lower-dimensional systems occur most likely within a shorter time interval, and all time intervals we chose as transients for the lower-dimensional systems were probably larger than necessary.

VII. TESTING FOR THE ROBUSTNESS AGAINST NOISE

To verify that our approach for estimating CLVs from data still yields useful results in the presence of noise, we estimated CLVs from trajectories of stochastic versions of the Lorenz attractor and the Lorenz 96 model. Uncorrelated Gaussian random numbers, drawn from distributions with standard deviations $\sigma = 1, 3$, and 5, are added to all three variables in the equations of the Lorenz attractor. For reference, the minimum and maximum values for the x , y , and z dimensions of this system are $-19.1, -26.2, 2.7$, and $18.9, 25.8, 46.8$. Comparing the range of these values (approximately 50) to the standard deviation of the added noise, we see, for example, that for $\sigma = 5$, the standard deviation of the added noise covers approximately 10% of the range of the variables. When processing the trajectories of the system with noise, we apply Savitzky–Golay filtering³¹ for the reconstruction of time derivatives before estimating Jacobians. As illustrated in Fig. 8, our approach still yields useful approximations of the Jacobians in the presence of noise. For the exact values of the LEs from data and from model-equations as well as their relative error, refer to Table I.

Nevertheless, the difference between equation-based Jacobians and estimated Jacobians as measured by Frobenius norms displays an offset that is clearly related to the applied noise strength. Note that the periodic fluctuations of the estimation error (best visible for $\sigma = 0$) can be well explained by the changes of the FTLE displayed in Fig. 2(e). Using these approximated Jacobians based on noisy data,

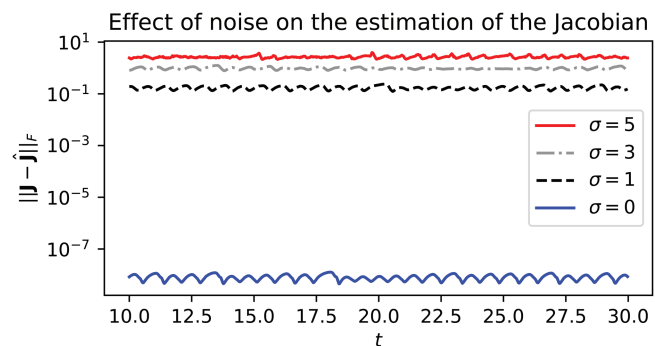


FIG. 8. The Frobenius norm of the difference between the actual J and approximated \hat{J} increases with the level of noise. Note that the y axis has a logarithmic scale. The introduction of noise has a noticeable effect on the estimation.

we compute CLVs, LEs, and FTLEs, which are presented in Fig. 9 for $\sigma = 5$. Data-based and equation-based CLVs for the stochastic Lorenz system are still tangent most of the time; however, deviations become more frequent under the influence of noise.

Additionally, we estimated histograms of the angles between data-based and equation-based CLVs, θ_i and ϕ_i , for various noise strengths. The resulting histograms are presented in Fig. 10. The absolute values of the cosines of angles between data-based and equation-based CLVs are unity for most time steps tested. Deviations from this value are more frequent if the vectors are computed using the NFM method, which is to be expected, since the NFM

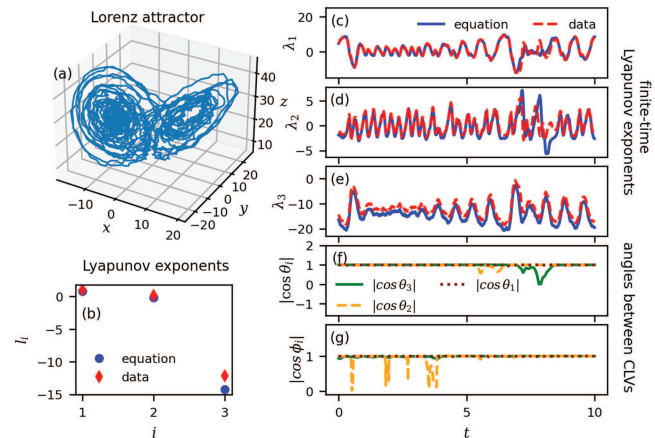


FIG. 9. Even in the presence of noise, we can obtain relatively accurate estimates of LEs, FTLEs, and CLVs. The panels above present the results for a stochastic version of the Lorenz attractor with the standard deviation of Gaussian white noise $\sigma = 5$. (a) Trajectory of the system. (b) LEs computed from model equations compared to LEs estimated from data. (c)–(e) Time series of data-based estimates of FTLEs compared to FTLEs computed from model equations. (f) Absolute value of the cosine of the angle between data-based and equation-based CLVs, both computed using Ginelli's algorithm. (g) Similar to (f) with both sets of CLVs estimated using the NFM.

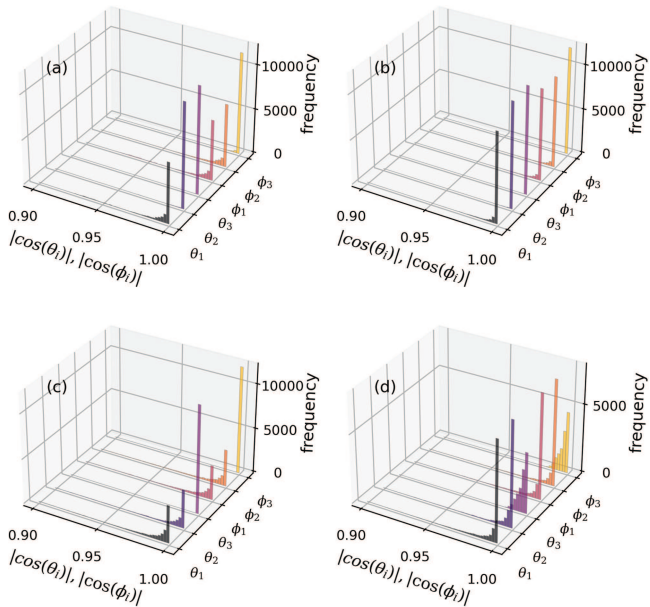


FIG. 10. Distribution of the absolute value of the cosine of the angles between data-based CLVs and CLVs obtained using model equations in a Lorenz attractor. (a) $\sigma = 0$, (b) $\sigma = 1$, (c) $\sigma = 3$, and (d) $\sigma = 5$.

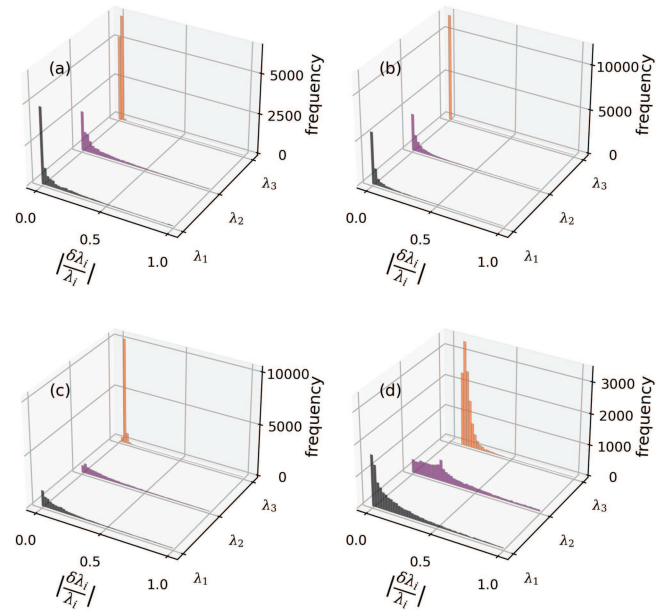


FIG. 11. Estimation error of FTLEs for a Lorenz attractor (a) $\sigma = 0$, (b) $\sigma = 1$, (c) $\sigma = 3$, and (d) $\sigma = 5$.

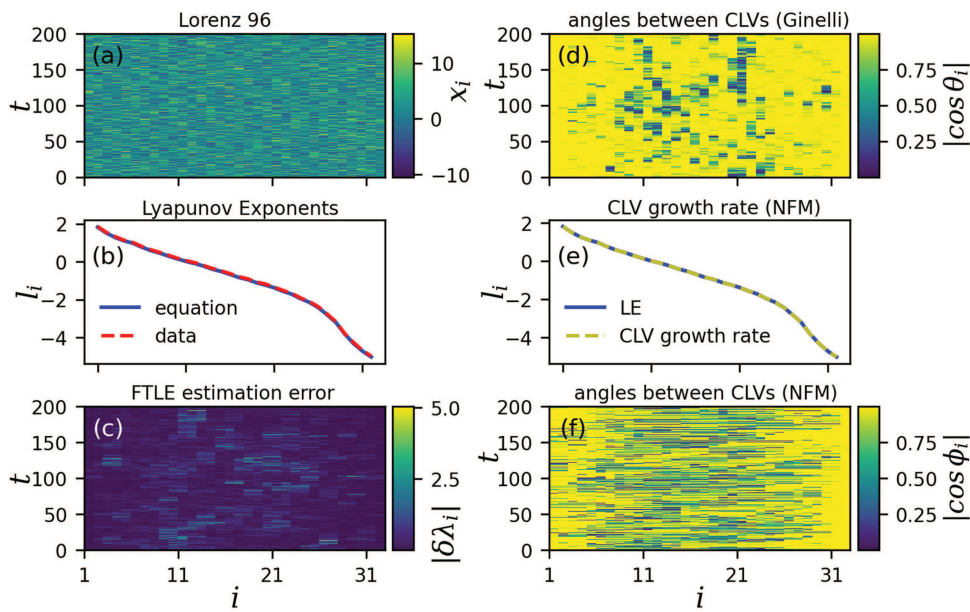


FIG. 12. Introduction of noise to a Lorenz 96 system with $n = 32$ and $F = 8$ decreases the accuracy of the estimated quantities. The Gaussian noise has a standard deviation of $\sigma = 0.5$. (a) Trajectories of the systems. (b) Data-based estimates of LEs compared to LEs computed from model equations. (c) Time series of the differences between data-based estimates of FTLEs and equation-based FTLEs. (d) Absolute value of the cosine of the angle between data-based and equation-based CLVs. Ginelli's method has been used to compute both sets of the CLVs. (e) LEs compared to the average growth rate of the CLVs estimated from the near future, both computed from model equations in order to test the NFM. (f) Similar to (d) with both sets of CLVs estimated using the NFM.

method represents an approximation to Ginelli's algorithm. We also observe an increased spread of the mass of the distributions when the noise strength is increased. This corresponds to the observations visible in the time series of Figs. 9(f) and 9(g) and the error growth of the Jacobian (see Fig. 8).

Analogously, histograms of relative differences of data-based FTLEs and equation-based FTLEs are presented in Fig. 11. The most frequent value of these differences is zero for $\sigma = 0$ and $\sigma = 1$. However, also, large differences occur (represented in the tail of the distributions) but are not very common. For $\sigma = 5$, we observe an offset of the distribution for λ_3 . One possible explanation for this could be that the measurement of shrinking perturbations along stable directions is more affected by the added noise than the measurement of growth along unstable directions. Growing perturbations most likely reach a magnitude that is much larger than the added noise after a few time steps, whereas shrinking perturbations apparently reach a magnitude that is comparable to the added noise. If the noise is increased, the most frequent value of relative differences shifts to a very small non-zero value and larger errors become more common. These observations correspond to the effects visible in the time series in Figs. 9(c)–9(e) and the error growth of the Jacobian (see Fig. 8). Additionally, we study the influence of noise on the Lorenz 96 system by adding Gaussian random variables to each iteration of the equations (4), i.e., a stochastic version of the Lorenz 96 system. The variance of the distribution from which the random variables are drawn is 0.5 for the results presented in Fig. 12. In contrast to the low-dimensional system, applying simple noise-filters in a pre-processing step does not improve the results. That is why the results presented here are generated without any previous noise filtering. The LEs can still be estimated well, even in the presence of noise. The estimation of CLVs shows, however, more errors for CLVs related to LEs that are close to zero. This is not surprising since these marginally stable directions are also difficult to compute from equations; i.e., typically some fine-tuning of the interval between QR decompositions is needed. This effect is less visible using Ginelli's method and more prominent for the approximative NFM. It is likely that some fine-tuning of the parameters of both algorithms (particularly, the time interval between QR decompositions) could improve the results. Nevertheless, the results presented here are generated using both algorithms as they were applied to the Lorenz 96 system without noise. CLVs related to leading stable and unstable directions can, however, still be estimated well from noisy trajectories. To summarize, we see an influence of the added noise on the quality of the estimates, and this influence becomes stronger when the noise strength is increased.

VIII. CONCLUSIONS

In this contribution, we propose an approach for estimating CLVs of dynamical systems from data without knowing the model-equations of the system. To obtain data-based estimates of Jacobians, we use the SINDy algorithm, a method for estimating model equations. For testing purposes, the data records are simulations of low- and high-dimensional nonlinear systems with and without noise. In this proof-of-concept study, we demonstrate that the estimated Jacobians can be used to generate reliable estimates of various characteristic quantities for the analysis of local stability

in dynamical systems, such as LEs, FTLEs, and CLVs. Comparing data-based estimates with quantities computed from the equations yields results that are almost indistinguishable in the absence of noise.

In the case of the Lorenz attractor, the presence of noise affects the quality of the results; more noise, as expected, makes the estimates more challenging. As discussed in Sec. VII, estimated LEs, FTLEs, and CLVs and their equation-based counterparts differ; yet, the estimated quantities are still able to reproduce qualitative behavior regarding the dynamics of the underlying system. Additional preprocessing steps can easily be coupled with our approach, as we demonstrated with applying Savitzky–Golay filtering to the stochastic version of the Lorenz attractor. Combining our approach with more sophisticated denoising methods during the preprocessing might yield even better results. Increasing the dimensionality of the spatiotemporal chaotic Lorenz 96 model had a minor effect on the quality of the results. Studying a stochastic version of the Lorenz 96 model revealed a more pronounced influence of the noise though. Whereas leading stable and unstable directions can still be estimated well, marginally stable directions become difficult to estimate.

In contrast to Ref. 13, the approach we propose is not based on phase-space reconstruction and can, therefore, be generalized to high-dimensional multivariate data records. The data needed to reconstruct phase-spaces scale exponentially with the dimension of the system, whereas the data-requirements of SINDy are determined by the regression tasks. Therefore, we can assume that the method proposed here needs considerably less data. As reported in Ref. 28, the amount of data necessary to discover the equations does, however, depend on the type of system that is studied and the variant of SINDy that is used. The runtime, furthermore, depends on the size of the library, which has to be chosen and also depends on the type of system under study. Note, however, that the algorithms to compute CLVs in high-dimensional dynamical systems require long-transients for the initial perturbations to converge. Approaches based on phase-space reconstruction can, though, address (low-dimensional) applications in which variables cannot be observed directly. The question how missing variables, less resolution in sampling, and missing data would influence the quality of all estimates has not been addressed in this proof-of-concept study but could be investigated in future contributions.

In summary, we propose a new method for estimating Jacobians from the time series of arbitrarily high-dimensional dynamical systems, and the quality of these estimates is sufficient to compute covariant Lyapunov vectors without knowing the model-equations. Being able to estimate covariant Lyapunov vectors on the basis of data records opens up the possibility of several applications, including prediction of critical transitions and studying perturbation growth on the basis of data records.

ACKNOWLEDGMENTS

The authors of this study are grateful to the BMBF for financial support within the project DADLN (No. 01|S19079) and to the Landesforschungsförderung Hamburg for financial support within the project LD-SODA (No. LFF-FV90).

AUTHOR DECLARATIONS**Conflict of Interest**

All authors declare that they have no conflicts of interest.

DATA AVAILABILITY

The data that support the findings of this study are available from the corresponding author upon reasonable request.

REFERENCES

- ¹A. Trevisan and F. Pancotti, "Periodic orbits, Lyapunov vectors, and singular vectors in the Lorenz system," *J. Atmos. Sci.* **55**, 390–398 (1998).
- ²D. Pazó and J. M. López, "Characteristic Lyapunov vectors in chaotic time-delayed systems," *Phys. Rev. E* **82**, 056201 (2010).
- ³H. L. Yang, K. A. Takeuchi, F. Ginelli, H. Chaté, and G. Radons, "Hyperbolicity and the effective dimension of spatially extended dissipative systems," *Phys. Rev. Lett.* **102**, 074102 (2009).
- ⁴K. A. Takeuchi, H.-L. Yang, F. Ginelli, G. Radons, and H. Chaté, "Hyperbolic decoupling of tangent space and effective dimension of dissipative systems," *Phys. Rev. E* **84**, 046214 (2011).
- ⁵M. W. Beims and J. A. Gallas, "Alignment of Lyapunov vectors: A quantitative criterion to predict catastrophes?" *Sci. Rep.* **6**, 37102 (2016).
- ⁶N. Sharifi, M. Timme, and S. Hallerberg, "Critical transitions and perturbation growth directions," *Phys. Rev. E* **96**, 032220 (2017).
- ⁷D. Pazó, M. A. Rodríguez, and J. M. López, "Spatio-temporal evolution of perturbations in ensembles initialized by bred, Lyapunov and singular vectors," *Tellus A* **62**, 10–23 (2010).
- ⁸S. Schubert and V. Lucarini, "Covariant Lyapunov vectors of a quasi-geostrophic baroclinic model: Analysis of instabilities and feedbacks," *Q. J. R. Meteorol. Soc.* **141**, 3040–3055 (2015).
- ⁹C. L. Wolfe and R. M. Samelson, "An efficient method for recovering Lyapunov vectors from singular vectors," *Tellus A* **59**, 355–366 (2007).
- ¹⁰D. Pazó, I. G. Szendro, J. M. López, and M. A. Rodríguez, "Structure of characteristic Lyapunov vectors in spatiotemporal chaos," *Phys. Rev. E* **78**, 016209 (2008).
- ¹¹F. Ginelli, P. Poggi, A. Turchi, H. Chaté, R. Livi, and A. Politi, "Characterizing dynamics with covariant Lyapunov vectors," *Phys. Rev. Lett.* **99**, 130601 (2007).
- ¹²P. V. Kuptsov and U. Parlitz, "Theory and computation of covariant Lyapunov vectors," *J. Nonlinear Sci.* **22**, 727–762 (2012).
- ¹³H.-L. Yang, G. Radons, and H. Kantz, "Covariant Lyapunov vectors from reconstructed dynamics: The geometry behind true and spurious Lyapunov exponents," *Phys. Rev. Lett.* **109**, 244101 (2012).
- ¹⁴A. Blanchard and T. P. Sapsis, "Learning the tangent space of dynamical instabilities from data," *Chaos* **29**, 113120 (2019).
- ¹⁵S. L. Brunton, J. L. Proctor, and J. N. Kutz, "Discovering governing equations from data by sparse identification of nonlinear dynamical systems," *Proc. Natl. Acad. Sci. U.S.A.* **113**, 3932–3937 (2016).
- ¹⁶E. N. Lorenz, "Deterministic nonperiodic flow," *J. Atmos. Sci.* **20**, 130–141 (1963).
- ¹⁷E. Neumann and A. Pikovsky, "Slow-fast dynamics in Josephson junctions," *Eur. Phys. J. B* **34**, 293–303 (2003).
- ¹⁸E. N. Lorenz, "Predictability: A problem partly solved," in *Seminar on Predictability* (European Centre for Medium-Range Weather Forecast, 1996), Vol. 1.
- ¹⁹M. Sano and Y. Sawada, "Measurement of the Lyapunov spectrum from a chaotic time series," *Phys. Rev. Lett.* **55**, 1082–1085 (1985).
- ²⁰J. P. Eckmann, S. O. Kamphorst, D. Ruelle, and S. Ciliberto, "Lyapunov exponents from time series," *Phys. Rev. A* **34**, 4971–4979 (1986).
- ²¹U. Parlitz, "Identification of true and spurious Lyapunov exponents from time series," *Int. J. Bifurc. Chaos* **02**, 155–165 (1992).
- ²²M. T. Rosenstein, J. J. Collins, and C. J. De Luca, "A practical method for calculating largest Lyapunov exponents from small data sets," *Phys. D* **65**, 117–134 (1993).
- ²³T. D. Sauer, "Formulas for the Eckmann-Ruelle matrix," in *Nonlinear Dynamics and Statistics*, edited by A. I. Mees (Birkhäuser Boston, Boston, MA, 2001), pp. 323–336.
- ²⁴A. Tanter, V. Lucarini, F. Lunkeit, and H. A. Dijkstra, "Crisis of the chaotic attractor of a climate model: A transfer operator approach," *Nonlinearity* **31**, 2221–2251 (2018).
- ²⁵B. Fornberg, "Generation of finite difference formulas on arbitrarily spaced grids," *Math. Comput.* **51**, 699–706 (1988).
- ²⁶L. Zhang and H. Schaeffer, "On the convergence of the SINDy algorithm," *Multiscale Model. Simul.* **17**, 948–972 (2019).
- ²⁷R. Tibshirani, "Regression shrinkage and selection via the lasso," *J. R. Stat. Soc. Ser. B Stat. Methodol.* **58**, 267–288 (1996).
- ²⁸K. Kaheman, J. N. Kutz, and S. L. Brunton, "Sindy-pi: A robust algorithm for parallel implicit sparse identification of nonlinear dynamics," *Proc. R. Soc. A* **476**, 20200279 (2020).
- ²⁹G. Benettin, L. Galgani, A. Giorgilli, and J.-M. Strelcyn, "Lyapunov characteristic exponents for smooth dynamical systems and for hamiltonian systems: a method for computing all of them. Part 1: Theory," *Mecchanica* **15**, 9–20 (1980).
- ³⁰N. Berglund and B. Gentz, *Noise-Induced Phenomena in Slow-Fast Dynamical Systems: A Sample-Paths Approach* (Springer Science & Business Media, 2006).
- ³¹A. Savitzky and M. J. Golay, "Smoothing and differentiation of data by simplified least squares procedures," *Anal. Chem.* **36**, 1627–1639 (1964).